Improving cellular uptake and cytotoxicity of chitosan-coated poly(lactic- co -glycolic acid) nanoparticles in macrophages

Article Body Template

PLEASE DO NOT INCLUDE ANY IDENTIFYING INFORMATION IN THE MAIN BODY OF THE MANUSCRIPT

- **Abstract:** <120 words. For research manuscripts, please include a structured abstract (i.e., Background, Materials & Methods, Results and Conclusion sections). For authors presenting the results of clinical trials, the guidelines recommended by CONSORT should be followed when writing the abstract (http://www.consort-statement.org/), and the clinical trial registration number included at the end of the abstract, where available. No references should be cited in the abstract.

Aim: This research aims to identify important formulation parameters for the enhancement of nanoparticle uptake and decreasing the cytotoxicity in macrophages.

Materials and methods: Fluorescent poly(lactic-co-glycolic acid) (PLGA) nanocarriers were characterised for size distributions, zeta potential and encapsulation efficiency. Incubation time, size class, PLGA derivative and chitosan derivative were assessed for uptake kinetics and cell viability.

Results: The major determining factor for enhancing cellular uptake were chitosan coatings, combined with acid-terminated PLGA and small nanoparticle size.

Moreover, cytotoxicity was more favourable for small, chitosan glutamate-coated, acid-terminated PLGA nanoparticles compared to its plain chitosan-coated counterparts.

Conclusion: Chitosan glutamate has been shown to be a valuable alternative coating material for acid-terminated PLGA nanoparticles to efficiently and safely target macrophages.

- **Lay abstract:** optional – a summary of the article with any technical jargon removed – the aim of these is to make an article more accessible and discoverable by readers who might not be experts in the field but have an interest in the topic – this can include anyone, but lay abstracts are particularly useful for patients and patient advocates, for example.

N/A

- **Graphical abstract:** optional – a concise, visual summary of the main findings of the article, helping readers to quickly understand the findings of the paper and its relevance to them.

Article Body Template

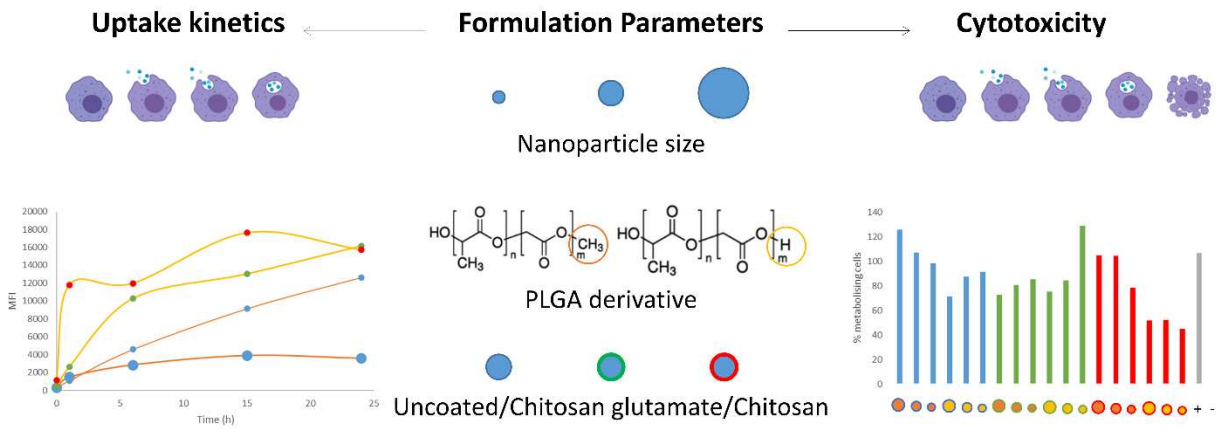

- **Video abstract:** optional – if the authors wish, they can provide a short video summary of their article (2–3 mins in total). Please provide a transcript of your video script, ideally prior to filming, so this can be peer reviewed alongside your article.

N/A

- **Tweetable abstract:** optional – if the authors wish, they can provide a tweetable abstract for the Journal Editor to use when sharing their article via social media, summarizing the key message of the article and including any relevant hashtags. Tweets can be up to a maximum of 280 characters, however we recommend ~200 characters for a tweetable abstract.

Due to their phagocytic nature, macrophages are attractive nominees for particle-based drug delivery systems. Some studies have shown benefits from chitosan-coated poly(lactic-co-glycolic acid) (PLGA) nanoparticles targeting macrophages; however, cytotoxicity is often considered an inconvenience.

This research aims to identify important formulation parameters for the enhancement of PLGA nanoparticle uptake in macrophages and decrease in cytotoxicity.

PLGA nanocarriers were characterised for size distributions, zeta potential and encapsulation efficiency. Incubation time, size class, PLGA derivative and chitosan derivative were assessed for uptake kinetics and cell viability.

The major determining factor for enhancing nanoparticle uptake were chitosan coatings, combined with the acid-terminated PLGA derivative and small nanoparticle size. The uptake rate was mainly elevated through coating with plain chitosan and larger particle size.

Cytotoxicity was more favourable for small, chitosan glutamate-coated, acid-terminated PLGA nanoparticles compared to its larger-sized, uncoated and plain chitosan coated counterparts. Overall, formulations based on ester-terminated PLGA nanoparticles showed the least toxic properties.

In conclusion, chitosan glutamate has been shown to be a valuable alternative coating material for small-sized acid-terminated PLGA nanoparticles to efficiently and safely target macrophages.

- **Keywords:** 5—10 keywords that encapsulate the scope of the article.

Poly(lactic-co-glycolic acid), PLGA, chitosan, chitosan glutamate, nanoparticles, macrophage, uptake, cytotoxicity, degradation

- **Main body of text:** for research manuscripts, please split this into i.e., Introduction, Materials & Methods, Results and Discussion/Conclusion sections.

1. Introduction

Macrophages are an important component of the innate immunity. Their role in several physiological and pathological processes has been studied thoroughly. Even though their biology has not been cleared up completely, it is known that macrophages exert various functions throughout the body. Therefore, macrophages are attractive candidates as therapeutic targets [1]. Furthermore, their phagocytic properties make them ideal nominees for particle-based drug delivery [2].
For instance, macrophages play a role in pathogen uptake, processing, elimination and antigen presentation. Therefore, they are suited targets for particle-based vaccine strategies [3,4].
Moreover, some pathogens escape lysosome digestion and can survive and proliferate inside the cell. *Mycobacterium tuberculosis*, *Leishmania donovani*, Human Immunodeficiency Virus (HIV), etc. are examples of pathogens that use macrophages as a shelter, resulting in chronic diseases that are difficult to treat. Patients might benefit from a particle-based drug delivery system containing specific antibiotic or antiviral drugs to eliminate these intracellular pathogens [5–9].
In addition, macrophages are known to migrate and accumulate in inflamed or infected tissue, at tumour sites and in epithelial barriers. While traveling to the site of action, they are able to transfer their cargo to and deliver the content at the site of action, which is a characteristic that can be exploited in inflammatory diseases and cancer [10–12].

In the past, macrophages have been regarded as an inconvenience as most of the administered particles are being cleared immediately by these cells of the reticuloendothelial system and barely reach the site of action [13]. However, when exploiting this phenomenon as a passive targeting strategy of macrophages, it is important to examine and optimize the effect of specific particle-characteristics on the uptake.
Shape, size and surface properties of the particles are described to have a relevant influence on the intracellular uptake. For example, spherical particles, nanoparticles and electrically charged particles are mentioned to be taken up preferably over rod-shaped or irregular particles, microparticles, and neutrally charged particles in alveolar macrophages. Moreover, enhancing particle-uptake could be established by hydrophobic, rigid, insoluble composition and smooth particle-surface [14,15].

The purpose of this study is to evaluate a non-toxic particulate drug delivery system with enhanced uptake-properties for different applications in macrophage-related diseases. One of the most commonly used materials in particulate drug systems is poly(lactic-co-glycolic acid) (PLGA), a polymer consisting of the metabolites glycolic acid and lactic acid. Depending on the ratio of both substances, release

properties can be altered. PLGA is considered to be safe (GRAS), biocompatible and biodegradable and is approved by the FDA for human use [16].
Another major advantage is, the possibility to encapsulate numerous of active pharmaceutical ingredients (API) into PLGA particles [17] using different techniques such as nanoprecipitation, spray-drying and the (double) emulsion solvent evaporation technique, the latter which was used in this research for nanoparticle production.
Moreover, PLGA allows manipulation of surface properties, e.g. ester end-capping, conjugation of ligands such as antibodies and coating by means of adsorption of other polymers. This provides different functionalities such as downgrading particle uptake in macrophages by polyethylene glycol-coatings and creating stealth nanoparticles (NPs) with a hydrophilic outer layer to avoid opsonisation and consequently (partial) macrophage-uptake through macrophage receptors [14].
Chitosan, in contrast, can be used as a coating material for PLGA NPs to modify surface properties from anionic to cationic. Chitosan is a sugar-like polymer and has biocompatible, biodegradable and mucoadhesive characteristics [18]. Additionally, chitosan coatings alter the release profile of PLGA NPs which becomes pH-dependent [3]. While chitosan coatings clearly have some functional benefits and enhance nanoparticle uptake [19], the downside is the potentially increased toxicity [20,21].

In this study, two derivatives of chitosan were compared as coating material for PLGA NPs. Since commonly used chitosan is associated with cellular toxicity, a chitosan glutamate derivative, previously shown not to be cytotoxic, was used [22].
Several characteristics that may affect intracellular uptake kinetics were evaluated through fluorescently labelled NPs; the choice of PLGA polymer (acid end-capped vs ester end-capped); uncoated versus chitosan (glutamate) coated nanoparticles; small versus medium versus large sized particles, as well as the incubation time. The effect of these parameters on the degradation properties of the NPs was evaluated by determining the intracellular fluorescence signals over a week. Finally, a resazurin cell viability assay was performed to determine the impact of these parameters on the cytotoxicity. Cultures of primary mouse macrophages were used for the *in vitro* screening of all formulations instead of the generally used RAW 264.7 or J774A macrophage cell lines for more relevant results.

2. Materials and methods

2.1 Materials

PLGA: Resomer® RG 503 (polymer P or 'P') [lactide:glycolide 50:50, ester-terminated, MW 24 000 – 38 000] was purchased from Evonik (Darmstadt, Germany) as for Resomer® RG 503 H (polymer H or 'H') [lactide:glycolide 50:50, carboxyl-terminated, MW 24 000 – 38 000] was produced by Boehringer Ingelheim (Ingelheim am Rhein, Germany). Chitosan glutamate (Cglu): Protasan UP G113® [MW 50 000 – 150 000, 75 – 90% deacylated] was provided by Novamatrix (Sandvika, Norway). Ethylacetate, polyvinylalcohol (PVA) [MW 31 000 – 50 000, 87-89% hydrolysed], chitosan (CHIT) [CAS 9012-76-4, 86% deacetylated], resazurin, Fluoroshield® and Triton X® were provided by Sigma-Aldrich (Overijse, Belgium). LPS-free water, disodium hydrogen phosphate dehydrate, sodium dihydrogen phosphate dehydrate and paraformaldehyde were bought from Merck GmbH (Overijse, Belgium). Fluorescein isothiocyanate (FITC), cell reagents (RPMI cell medium, Accumax® etc.), Texas Red-X phalloidin were purchased from Thermo Fisher Scientific (Merelbeke, Belgium). Acetic Acid, ammonium-chloride-potassium lysis buffer were obtained from VWR international (Leuven, Belgium), mannitol from Duchefa Farma (Haarlem, The

Netherlands), sodium hydroxide 0.1 M solution from Fluka, Sigma Aldrich (Overijse, Belgium) and sodium chloride from Carl Roth GmbH (Karlsruhe, Germany).

2.2 Methods

2.2.1 Preparation of nanoparticles

Three replicas of PLGA NPs of both polymers P and H were prepared by means of the water-in-oil-in-water (W/O/W) double emulsion solvent evaporation method, followed by washing and freeze-drying for long term storage. FITC was encapsulated as a fluorescent marker.
Firstly, 500 mg of PLGA was dissolved in 5 mL of ethyl acetate. Then, FITC was dispersed in phosphate buffered saline at a final concentration of 1 mg/mL. 1 mL of the water phase was added to 5 mL of the organic phase and emulsified by ultrasonication (1 minute, amplitude 20%) (VIBRA CELL VCX-750, 6 mm probe, Sonics, USA). This W/O emulsion was added to 10 mL of an external water phase containing either 0.1%, 0.4% or 1% (w/w) PVA as a stabiliser and emulsified by ultrasonication (1 minute, amplitude 20%) in order to vary the size of the NPs. The resulting W/O/W emulsions were diluted with 30 mL of the corresponding PVA solution and magnetically stirred (500 rpm) at room temperature for 24 h to allow the evaporation of the solvent.
The produced nanoparticles were washed three times using centrifugation (9000x g or 20 000x g for 30 minutes) (Sigma 4-16 KS, Sigma Laborzentrifugen GmbH, Germany) to remove PVA and divided into three groups. A coating solution of either 0.6% (w/w) Cglu in water or 0.6% (w/w) CHIT in 1% (w/w) acetic acid was added to two out of three groups, where the third group was left uncoated (NC). NPs were magnetically stirred overnight at room temperature and washed three times using centrifugation to remove unadsorbed coating material. Finally, the particles were added to 1 g mannitol as a cryoprotectant, lyophilized for at least 72 h (FreeZone 1 liter benchtop freeze dry system, Labconco, USA) and stored at 2 – 8 °C in an airtight plastic container protected from light until further use.

2.2.2 Characterisation of nanoparticles

2.2.2.1 Yield

The yield (particle concentration, expressed as mass PLGA per mass freeze-dried powder in percentage) of each sample was calculated by weighing samples after freeze drying, taking the amount of mannitol added prior to freeze drying, into account.

2.2.2.2 Scanning electron microscopy

The morphology of the NPs was determined with scanning electron microscopy (SEM).
An amount of 100 mg of freeze-dried sample was weighed and reconstituted in 1 ml ultrapure water. Mannitol was washed of through centrifugation (9000x g for 10 or 30 minutes). The PLGA pellet was reconstituted in 1 mL of ultrapure water, sonicated for 15 min and vortexed extensively. Then, 10 µL of the NP dispersion was spotted on a membrane filter. A gold layer of 10 nm was applied with a sputter coater and the sample was dried in a desiccator for 45 min at room temperature. Imaging was carried out with a Jeol JSM-IT100 microscope (Jeol, Japan).

2.2.2.3 Nanoparticle size distribution analysis

NP size distributions of freeze-dried samples were measured in ultrapure water using a laser diffraction particle size analyser (Mastersizer 3000, Malvern Instruments, United Kingdom). An average of 5 measurements for each sample was calculated. Results were expressed as Number Density (%) in function of size and size distributions were defined by dx(10), dx(50) and dx(90), being the particle diameters accumulated number ratio of 10%, 50%, and 90%, respectively. The span index of NP size distributions was also evaluated as a measure for the width of the distribution.

2.2.2.4 Zeta potential analysis

Zeta potential was determined through electrophoretic light scattering (Zetasizer 2000, Malvern Instruments, United Kingdom). Measurements were carried out in ultrapure water and results were calculated as the average of three measurements for each sample.

2.2.2.5 Encapsulation efficiency

The encapsulation efficiency of FITC was analysed through a spectrophotometric assay (Specord 200 plus, Analytik Jena AG, Germany). The FITC standard curve in 0.1 M NaOH showed good linearity (R^2 > 0.999), linear range was 0.0005 mg/mL to 0.005 mg/mL measured at 490 nm wavelength.
An equivalent amount of freeze-dried sample containing 4.8 mg of PLGA NPs was accurately weighed, reconstituted in 1 ml 0.1 M NaOH solution and vortexed for 1 minute. After 2 hours,
FITC containing aqueous solution was collected with the aid of centrifugation (9000x g for 10 or 30 minutes) and measured at 490 nm. Each batch was measured in triplicate.
The encapsulation efficiency (EE) in the nanoparticle formulations was determined employing the following equation:

$$EE\ (\%) = \frac{Measured\ amount\ of\ FITC}{Theoretical\ amount\ of\ FITC} * 100\%$$

The dye loading (DL) is defined as

$$DL\ (\%) = \frac{Measured\ amount\ of\ FITC}{Weighed\ amount\ of\ PLGA\ NPs} * 100\%$$

2.2.3 Phagocytosis experiments

2.2.3.1 Ethical statement

Cells were collected from leftovers of sacrificed control female Swiss mice, from experiments authorized by the Ethical Committee for Animals of the University of Antwerp; permit numbers 2011-74 and 2019-10.

2.2.3.2 Collection of cells

Primary bone marrow-derived macrophages from two to three female Swiss mice were collected by flushing the tibia with RPMI medium. After removing red blood cells with an ammonium-chloride-

potassium lysis buffer, macrophages were counted and seeded in a 24-well plate at a concentration of 2 x 10^5 cells/well. RPMI cell medium enriched with 10% iFBS, 1% non- essential amino acids, 1% sodium pyruvate, 1% glutamine and 10% L929 supernatant was added after 4 to 6h and refreshed after another 24 hours and 3 days of incubation time. L929 cells were kindly provided by Dr. C. Uyttenhove (Ludwig Institute for Cancer Research, Brussels, Belgium). Macrophages were cultured for 7 days in total before phagocytosis experiments were performed.

2.2.3.3 Uptake kinetics

NPs were reconstituted in ultrapure water and washed by through centrifugation at 9000 x g during 10 or 30 minutes. Cooled enriched RPMI cell medium was added to the NPs after which they were sonicated for 15 minutes to enhance reconstitution in medium. 300 µL of 2.7 mg/mL of NPs was added to the cells after 7 days of maturation and incubated at 37°C. At specified time intervals (0, 1, 6, 15 and 24 hours), cells were washed three times with PBS, partially dissociated with Accumax® for 30 minutes, fixed with 4% (w/v) paraformaldehyde and detached from the plate with a cell scraper for flow cytometry analysis. The experiment was performed once on replica I and thrice on replica's II en III.

2.2.3.4 Intracellular FITC signal over time

The stability of the FITC signal inside the cells was determined to evaluate controlled release of the dye inside the cell. An amount of 300 µL of a 2.7 mg/mL NP dispersion was added to the cells after 7 days of maturation and incubated at 37°C. After 6 hours (saturation phase for most formulations), cells were washed three times with cell medium and incubated further at 37°C. At specified time intervals (24, 72, 168 hours), cells were washed three times with PBS, partially dissociated with Accumax® for 30 minutes, fixed with 4% (w/V) paraformaldehyde, detached from the plate with a cell scraper and analysed using flow cytometry. The outcome, reduction in MFI, was calculated as the difference between the maximum FITC signal after incubation of cells with NPs and the FITC signal at the endpoint of 7 days. The experiment was performed thrice, once on each replica.

2.2.3.5 Flow cytometry

The fluorescence of cells was measured utilising an Attune NxT Flow Cytometer (Thermo Fisher Scientific, Singapore), with excitation from a blue laser (488 nm) and detection through FSC, SSC and the first fluorescent channel (BL1). Outcomes were Mean Fluorescence Intensity (MFI) as a measure for cellular NP-uptake and the number of fluorescent cells (%) (cut-off value of a 'fluorescent cell': MFI > 2 x 10^3 (Fig. S1).

2.2.3.6 Fluorescence microscopy

Cells were seeded in 96-well plate suited for imaging in a concentration of 2 x 10^4 cells/well. NPs were added in a concentration of 2.7 mg/mL, cells were incubated at 37°C for 0, 1 and 6 hours. To control whether NPs were taken up through passive diffusion and assess adhesion of NPs to cells, the experiment was also done at 4°C to inhibit active transport. Macrophages were then washed three times with PBS, fixed with 4% paraformaldehyde, permeabilised with Triton-X®, coloured with phalloidin-Texas Red-X to visualise the cell filaments and Fluoroshield® containing 4',6-diamidino-2-phenylindole

(DAPI) to stain cell nuclei. Fluorescent images were obtained with an Axio Observer inverted microscope connected to a Compact Light Source HXP 120C with Filter set 49, 20 and 10 for blue, red and green fluorophores respectively (Carl Zeiss Microscopy, Germany).

2.2.3.7 Cytotoxicity study

A resazurin cell viability assay was performed to verify NP toxicity. Macrophages were incubated with the high-rated concentration of 2.7 mg/mL NPs in a 96-well plate containing 3 x 10^4 cells/well. After 0, 1, 6 and 24 hours, cells were washed three times with PBS and 200 µL of enriched RPMI cell medium was added and 50 µL resazurin solution was added to the cells. After 4 h incubation time at 37°C, the MFI of the fluorescent metabolite resorufin was measured at 590 nm using a Tecan GENios microplate reader (Tecan, Switzerland). A standard curve of a 50% serial dilution was assembled to calculate the number of metabolising cells (cell viability) (%).

2.2.4 Statistical analysis

Results of nanoparticle characteristics were calculated as the mean, followed by the standard deviation. For uptake kinetics, a mixed linear regression model (R) was fitted and the effect of the following parameters: incubation time, nanoparticle size class, PLGA polymer type and surface coating, as well as the interaction effects between these parameters, corrected for dye loading as a covariate, on the outcomes MFI and the number of fluorescent cells (%), was assessed. Since incubation time wasn't showing a linear relationship with the outcomes, it was included as a categorical covariate in the model. 2-way ANOVA analysis was performed for further analysis of the parameters size class, polymer type and surface coating, taking dye loading into account as a covariate. The difference in uptake between the start and the endpoint of the experiment was the dependent variable.
For intracellular stability and cytotoxicity, a multiple linear regression model (SPSS) including nanoparticle size class, polymer and coating, was used to identify significant parameters and/or interaction effects. At last for cytotoxicity, cell viability of the different formulations was also compared to the positive control group by means of an unpaired two-tailed student t-test. P-values smaller than 0.05 were considered significantly different.

3. Results

3.1 Nanoparticle characteristics

3.1.2 Scanning electron microscopy

SEM pictures (Fig. 1, Fig. S2) revealed spherical shaped nanoparticles in all samples. When increasing the concentration of stabiliser in the outer water phase during production, NPs became smaller. For samples produced with 0.1% PVA in the second water phase, a minority of micro-range sized particles were observed (Fig. 1 A, B, C). Samples are coded by three formulation parameters:
1. The amount of stabiliser used, indicating size class (0.1 – 0.4 – 1)
2. The PLGA polymer used, indicating polymer H (Resomer® RG 503 H) or P (Resomer® RG 503)
3. The surface properties, indicating uncoated (NC), chitosan glutamate-coated (Cglu) or chitosan-coated (CHIT) NPs

In all samples coated with CHIT, thread-like structures causing aggregation were noticed (Fig. 1 C, Fig. S2), which might be remaining polymeric chitosan remnants.

3.1.3 Nanoparticle size distributions

As mentioned before, the higher the concentration of PVA, the smaller the NPs. Interestingly, the span index, balanced around 1 in all formulations, no matter the polymer or concentration of stabiliser, which corresponds to monodisperse nanoparticle size distributions. Although applying the same above-mentioned production method, particles consisting of polymer P were significantly smaller (p-value 0.013) in a multiple linear regression model than those produced with polymer H, taking concentration PVA into account. The three nanoparticle replicas produced with polymer P showed good reproducibility in terms of nanoparticle size distribution diameters, likewise when coated with Cglu. Polymer H NPs showed higher variability between batches and consequently after chitosan coatings as well (Fig. S3, Fig. S4). Results are shown in Table 1.

3.1.4 Zeta potential measurements

As expected, evaluation of zeta potential measurements in ultrapure water showed negative values for NC NPs and positive values for Cglu- and CHIT-coated NPs. Results are presented in Table 1. Lower values for Cglu-coated NPs were observed compared to CHIT-coated NPs, especially when combined with polymer P.

3.1.5 Encapsulation Efficiency

Substantial differences in encapsulation efficiency (EE) were observed between formulations, even amongst replicas (Fig. S5), ranging between 4.2% and 33.3% of FITC. Results are shown in Table 1. Noteworthy is the fact that EE decreased when coating procedures were applied on NP formulations. The decrease due to diffusion of FITC out of the NPs was more extensive for Cglu (Polymer P: ± 40%, Polymer H: ± 60%) compared to CHIT (Polymer P: ± 20%, Polymer H: ± 30%).

3.2 Phagocytosis experiments

3.2.1 Uptake kinetics

3.2.1.1 Incubation Time

To study the effect of incubation time, nanoparticle size, polymer type and surface coating, linear mixed models were fitted. Overall, all parameters appeared to have a significant interaction effect with time on the uptake kinetics. This means that the course of the nanoparticle uptake profiles was different for all formulations over the observation period of 24 hours.
During the first hours of uptake a steep increase in MFI (Fig. 2) and number of fluorescent cells (Fig. 3) was observed. Therefore, during these first hours, the longer the nanoparticles were in contact with cells, the more nanoparticles were engulfed. During the first hour the steepest change in MFI for most combinations of parameters was observed. However, after 6 hours some formulations already reached their maximum, while others, e.g. small NPs, kept increasing.

It must be noted as well that fluorescent cells were already present on time point zero, where NPs were added to the cells and were washed off immediately. (Fig. 3) This phenomenon mainly occurred in CHIT coated NPs and was also present, to a lesser extent, in Cglu coated NPs. Similarly, the MFI was also slightly higher in coated nanoparticles compared to plain nanoparticles at time point zero. (Fig. 2)

3.2.1.2 Size Class

In general, we observed an inverse relationship between particle size and NP-uptake over time, where the smaller the NPs, the more preferable they were taken up over larger-sized NPs after 24 hours. (Fig. 2, Fig. S6) Because the two polymer types gave rise to substantial differences in particle size distributions, they were analysed independently. For both polymers H and P, there was no significant interaction between the parameters size class and surface coating, however both parameters did show a significant main effect in the model. For polymer H, Tukey post hoc testing revealed a significant higher uptake over 24 hours of small and medium-sized NPs compared to large NPs (resp. p-values: 0.031 and 0.013). For polymer P, small NPs were significantly more taken up in reference to large and medium-sized NPs (resp. p-values: 0.003 and 0.016).

3.2.1.3 Surface properties: polymer

When comparing the uptake profiles of uncoated formulations, the ester end-capped polymer resulted generally in higher uptake values compared to its acid-terminated complement (Fig. S6). However, dye loading and size distributions were not comparable for the two types of polymer and statistical analysis showed a significant interaction effect between polymer and size class. Therefore, the analysis was split between the three size classes and no significant difference in total uptake between polymer H and P existed.

3.2.1.4 Surface properties: chitosan coating

While the EE of coated nanoparticles was lower compared to uncoated NPs, their MFI uptake profiles and maximum amount of fluorescent cells showed to be systematically higher. (Fig. 2)
Chitosan coatings are thus a major determining factor in elevating nanoparticle uptake.
Considering the uptake profiles of Cglu NPs were laying between the ones from NC and CHIT NPs, it seemed that CHIT was superior over Clgu. However, Cglu NPs gave rise to a lower dye loading compared to CHIT.
2-way ANOVA with Tukey post hoc corrections showed for polymer H a significant higher uptake for both Cglu and CHIT compared to uncoated NPs (resp. p-values 0.0023 and 0.0009). No difference between Cglu and CHIT could be observed. For polymer P a modest significant higher uptake for CHIT compared to NC NPs (p-value 0.0489) was found. However, CHIT vs. Cglu and Cglu vs. NC were not significantly different from each other.

3.2.2 Fluorescence microscopy

In general, fluorescence images confirmed the effects observed in the uptake profiles obtained by flow cytometry. The images revealed absence of uncoated NPs at time point 0 hours at 37°C and time point 6 hours at 4°C, however, few chitosan (glutamate)-coated NPs attached to the cells were noticed at these

conditions. NP uptake profiles indicated high uptake rates during the first hours after which saturation was reached around 6 hours for large NPs. Fluorescence microscopy established this phenomenon for 0.1 H NC NPs, where cells were overfilled with NPs after 6 hours incubation time. In contrast, for smaller NPs (e.g. 1 P NC) the uptake profile kept increasing slowly during the observation period of 24 hours, pictures revealed no saturation of the cells after 6 hours incubation time, but a high amount of particles at 24 hours. After analysis of all uptake profiles, taking dye loading into account, the major determining factor in the enhancement of nanoparticle uptake is the change in surface properties due to chitosan coatings. Wherefore, CHIT coated NPs seem to have the fastest NP uptake (e.g. comparing fluorescence images of 0.4 H Cglu vs 0.4 H CHIT at 1 hour), but on the other hand, Cglu accordingly increased NP uptake and no significant difference could be determined between the two types of coating material over the observation period of 24 hours. (Fig. 4)

3.2.3 *In vitro* degradation properties

Compared to a FITC-control, where MFI decreased to the baseline after 48 h, all NP formulations presented fluorescent signals after 1 week of incubation. (Fig. 5) For plain nanoparticles, MFI decreased already after 24 hours, while for some Cglu and CHIT formulations the FITC-signal increased or was stable at first instance. Eventually all formulations had a decreased signal in the end. Similar profiles could be observed for the outcome number of fluorescent cells (Fig. S7).
Statistical analysis of percentage in reduction of MFI between the endpoint of the profiles compared to the maximum MFI, showed size class to be the only significant parameter (p-value 0.018). The overall reduction in MFI was 13.5% higher in large NPs in reference to small NPs. Coating and polymer were of no importance and were left out of the model. Noteworthy is the consistency in MFI reduction for Cglu NPs which was 40 – 50% for all formulations, independent of size class. (Fig. 6)

3.2.4 Cytotoxicity study

After 1 h (Fig. S8), a slight decrease in MFI for macrophages treated with polymer H CHIT-coated NPs was observed. This phenomenon became more outspoken after 6 h (Fig. S8) and 24 h (Fig. 7). Hence, a multiple linear regression model of % metabolising cells on the 24h time point showed a significant interaction effect (p-value 0.045) between surface properties and type of polymer on cell viability, indicating the above mentioned effect of cytotoxicity of polymer H NPs combined with plain chitosan. Another significant interaction effect (p-value 0.023) between size class and polymer was observed. A higher decrease in cell viability for 0.1 H NC and 0.1 H Cglu NPs compared to the small ones was found. No cytotoxic effect was observed for polymer P uncoated NPs, nor when combined with plain chitosan. Moreover, a higher amount of % metabolising cells was present for some of these groups compared to the positive control group. Unpaired two-tailed t-testing (SPSS) of all formulations compared to this positive control group, didn't indicate a significant difference for these 'activated' groups.

4. Discussion

After nanoparticle characterisation, the various polymers and coating materials resulted in differences in size distributions, zeta potential and loading efficiencies of the particles. While the production process was similar, particles consisting of polymer P were generally smaller compared to the ones consisting of polymer H. We hypothesised that for polymer H, the repulsion between deprotonated carboxylic end

groups at the surface of the inner water phase (PBS with pH 7.4) extended the emulsion droplets and therefore created larger nanoparticles after solvent evaporation. It has to be noted as well that chitosan-coatings may result in an increase in nanoparticle size [23]. For 1% PVA polymer P CHIT coated NPs (1 P CHIT), this effect was excessive. Several reasons could address this phenomenon, for instance, the washing procedure after coating through centrifugation was insufficient for such small particles in a highly viscous coating solution. Therefore, ultracentrifugation might have been more appropriate. Furthermore, uncoated nanoparticles were dispersed easily in ultrapure water after freeze-drying. Cglu-coated NPs required one or two cycles of 120 seconds sonication to eliminate agglomerates. CHIT NPs were very poorly dispersed as initial size measurements showed agglomerates ranging around several micrometres. Only after 4 to 7 cycles of 120 seconds of sonication in the system, measurements remained stable, meaning agglomerates were (partially) broken down. Due to the thread-like structures as seen on the SEM pictures, NPs were 'glued' together to bigger agglomerates which were difficult to separate. This was also observed, especially for 1 H CHIT NPs, with fluorescence microscopy. (data not shown) High concentrations of CHIT could induce multiple loosened chitosan layers onto the initial tight chitosan layer covering the NP surface. The upper layers consisted of coils or interacting chains [23]. Consequently, prior to all our other experiments sonication has been used to counter this inconvenience.

When analysing zeta potential measurements, Cglu NPs (especially P Cglu NPs) showed lower absolute values compared to CHIT-coated NPs and uncoated NPs. Therefore, P Cglu NPs may be colloidal less stable in aqueous media during long-term storage, as generally the cut-off value for stable colloidal dispersions is established at plus or minus 30 mV [24].

All formulations showed substantial differences in encapsulation efficiencies, even between replica's. We hypothesised that because FITC was dispersed in PBS due to low water solubility, this resulted in less homogeneous starting-material and therefore a feasible higher variation in EE. Moreover, the ratio dye/polymer of 1 mg/500 mg could only amount to a very low maximum dye loading of 0.2% (w/w), wherefore inequalities easily occurred. In general, the low EE could be expected when applying the W/O/W double emulsion solvent evaporation method [25]. Moreover, a trend of consequent leakage of dye out of the particles during the coating procedure was observed, which was higher for Cglu compared to CHIT. Probably, the higher viscosity and lower pH of CHIT solutions compared to Cglu solutions resulted in fewer dye loss. For uptake kinetics, the dye loading is considered to be an important covariate in the analysis model, as none of the preparations contained the same amount of FITC.

It is clear that nanoparticle uptake is time-dependent, as differences in uptake profiles were found. Slightly elevated MFI and fluorescent positive cells at time point zero suggest an interaction between positively charged amino-groups of chitosan and the negatively charged cell membrane adhering the NPs to the surface of the cells [26]. Fluorescence microscopy images confirmed an electrical interaction between cellular membrane and the positively charged NPs. Both at time point 0 hours at 37°C and time point 6 hours at 4°C, few chitosan (glutamate)-coated NPs attached to the cells were noticed. Uncoated NPs on the other hand were not visible, implying there was no interaction with the cellmembrane present for this type of NPs. (Fig. 4)

Lutsiak et al. studied PLGA nanoparticle uptake (NPs ± 500 nm) in macrophages (J774.A) and found that the number of phagocytic cells did not increase between 12 h and 24 h, but the MFI did, and maximal levels of phagocytosis were reached within 24 h. However, the difference in MFI between 1 h, 4 h and 8 h appeared to be higher compared to the 12 h time point, which is comparable to our results in uptake

kinetics [27]. Xiong et al. analogously saw the cellular uptake of PLGA NPs (± 118 nm) in RAW264.7 cells increasing with longer incubation time, but a gradual decline of cellular uptake speed over time was observed [28]. Overall, our data likewise revealed that nanoparticle uptake rates were high during the first hours and then the MFI either decreased, stabilised or increased, which depended on the nature of the formulation. The larger the NPs, the sooner a plateau phase or decrease in MFI was seen due to saturation of the cells, while the uptake profiles of smaller NPs kept increasing during the observation period and correspondingly the pace to reach the maximum value was slower for small-sized NPs.
On the other hand, total uptake after 24 hours was generally higher for small nanoparticles. This observation has already been established when comparing nano- and microparticles, nevertheless, the trend continued in our research focussing on the nanoscale size range.
Other studies determined that NPs of 100 – 200 nm were preferentially taken up over larger NPs (< 1 µm) in alveolar macrophages. Nonetheless, this tendency also seems to be limited, as very small NPs (< 100 nm) showed less opsonisation of plasma components and therefore a reduced uptake by the cells of the RES [14,29,30].
Remarkably, no difference in uptake between uncoated NPs consisting of both PLGA derivatives could be determined, although Resomer® RG 503 H contains deprotonated carboxylic acid groups (at physiological pH), which are prone to repulsion by the negatively charged cell membrane in contrast to the ester-terminated Resomer® RG 503 [13]. It has also been described that electrically charged NPs are preferably taken up by macrophages compared to neutrally charged NPs [31]. The zeta potentials were comparable for both types of uncoated NPs in ultrapure water, suggesting there wasn't an actual 'electrical charge' difference present. Moreover, the negative charge of carboxylic acid groups could be partially shielded by ions adsorbing to the surface of the nanoparticles, which is also the case for neutrally charged particles, even more in electrolyte-rich cell medium [22]. Therefore, ester end-capped and acid-terminated PLGA polymers might indeed not substantially influence the NP uptake properties compared to each other in primary murine macrophages. The reason for higher MFI values after uptake for polymer P compared to polymer H particles in Fig. 2 could be addressed to their smaller size and higher encapsulation efficiency.
The major determining factor enhancing nanoparticle uptake was found to be the coating of NPs with both chitosan derivatives. This has already been established in a few studies comparing positively charged NPs to negatively charged ones [19,26]. However, it appears that the core of the NPs, the polymer type, mattered as well in elevating NP uptake, which was more outspoken for polymer H compared to polymer P. Durán et al. showed that the mannose-receptor was upregulated after 2 hours and 24 hours incubation time in human antigen presenting cells when incubated with chitosan-coated NPs. Accordingly, active targeting of these cells was suggested, where chitosan was able to interact with the mannose-receptor and higher uptake was achieved [19]. However, because of the lack of experiments blocking the mannose receptor during nanoparticle exposure, a definite answer to this matter could not be provided. It should be noted that both MFI and amount of fluorescent cells were consequently higher for CHIT NPs after 1 hour incubation time compared to Cglu NPs, suggesting uptake rates were higher for this coating material independently of size class. Due to higher electrical charges (higher zeta potential), CHIT NPs might be taken up more effectively [31]. Nevertheless, at time point 24 hours, no difference in total nanoparticle uptake between H Cglu and H CHIT nanoparticles could be found.

As discussed earlier, chitosan coatings might alter release properties of nanocarriers [3]. However, out of our experiments, it can be concluded that coating of the NPs with either chitosan or chitosan

glutamate did not protect the core of the NPs and correspondingly FITC from degradation over time inside the cells. When analysing the degradation profiles, the drop in FITC signal of coated NPs did not occur immediately after nanoparticle removal. As mentioned before, Cglu and CHIT-coated NPs adhered to the outer cell surface. Therefore, cells were probably still able to ingest NPs after the washing step, resulting in stable or increased fluorescence 24 hours later. For uncoated NPs, polymer P showed prolonged stability compared to polymer H, which can be expected, as carboxyl-terminated PLGA is more prone to autocatalysis compared to ester-terminated PLGA [32]. Oppositely, for Cglu-coated NPs, polymer H seemed to show higher values compared to polymer P, because of additional uptake after 24 hours, but their curves were equally steep. Finally, profiles of CHIT NPs showed higher values for smaller polymer H compared to large NPs and polymer P NPs.

When focussing on the MFI reduction, Cglu-coated NPs showed a consistent decline, while uncoated and CHIT-coated larger NPs tended to have a higher reduction in MFI compared to medium-sized and small NPs. These results are the opposite of *in vitro* release studies performed on PLGA NPs, where small NPs with large surface area presented a quicker release of their cargo [33]. However, large NPs give rise to enhanced autocatalysis of the polymer [17]. Additionally, as larger NPs saturated cells more quickly, more degradation products were formed, leading to acidic pH values, hence, a drop in FITC signal due to degradation of the dye. For chitosan glutamate, acidification occurs as well in aqueous environment and as this promotes autocatalysis of the PLGA NPs, it is expected that chitosan glutamate too could contribute to steady NP degradation, even independent of NP size. Consequently, chitosan glutamate coatings allow a predictable sustained release profile.

Cellular toxicity was mainly found for larger NPs compared to small ones and when consisting out of Resomer® RG 503 H, whether or not coated. Van de Ven et al., designated the cytotoxic effect of PLGA NPs in a high dose to be related to the build-up of degradation products of the polymer inside the cell. Implying that the faster PLGA NPs degraded, the higher the cytotoxicity [34]. Our experiments support this hypothesis, as a difference in MFI reduction between polymer H and polymer P was present even during the short term of 24 hours, suggesting a more rapid degradation of polymer H, especially in large NPs.

As expected, Resomer® RG 503 NPs shows only slight cytotoxic effects and peculiarly this is also the case when coated with plain chitosan. Even though zeta potentials were similar to polymer H NPs, less electric interactions could have been established between the neutral polymer P and CHIT compared to the carboxyl end-capped polymer and consequently, fewer CHIT could have been adsorbed onto the surface, resulting in less cytotoxicity [23]. Furthermore, because chitosan glutamate possibly contributes to faster degradation of the PLGA polymer, it would explain the occurrence of cytotoxicity in Cglu-coated polymer P NPs.

Other studies confirmed our results [19,21], as for example: Duran et al. found that both PLGA NPs (Resomer® RG 503 H) and chitosan chloride-coated NPs (Protasan® UP CL 113) were toxic in concentrations of 600 µg/mL, causing 20 – 40% cell death respectively. Another study investigated chitosan microspheres which were demonstrated to be cytotoxic in J774.1 macrophages, opposed to PLGA microparticles. However, those PLGA microparticle-formulations did show some cytokine-production and inflammatory response [35]. It has been demonstrated that macrophages were activated after nanoparticle uptake [36,37] and phagocytic activity was stimulated as the number of particles taken up by individual cells had grown and the population of attracted macrophage cells risen [38]. This might explain the raise in number of metabolising cells for polymer P NC NPs in our experiments compared to the positive control group. To overcome the limitations of this technique, it

should be further investigated if and why changes in cellular metabolism occurred, especially in polymer P NPs, possibly complemented with death-life staining assays of the cells. This would provide better insight whether or not cytotoxicity also occurred in this type of particles. Accordingly, it would be interesting to address other limitations related to our work, such as the examination of changes in cellular biology e.g. phenotyping of the macrophages or researching cytokine release after nanoparticle exposure. Furthermore, co-localisation experiments to research the intracellular faith of the NPs could provide better understanding of their degradation profiles and their purpose in relation to their application as a drug delivery system. Although important, these issues transcended the aim of this screening study and will be approached in future experiments.

5. Conclusion

When developing nanocarriers for a certain purpose, important characteristics of these drug delivery systems should be considered. Effective nanoparticle uptake, as well as safety and controlled release properties are important requirements for particulate-based drug delivery systems. In this study, we assessed the influence of different formulation parameters of PLGA NPs on the uptake kinetics, degradation properties and cytotoxicity in macrophages.

A major enhancement in nanoparticle uptake resulted from altering the surface properties of PLGA NPs, especially when consisting of Resomer® RG 503 H, by chitosan coatings. Therefore, active targeting; e.g. of the mannose receptor, is preferable for macrophage drug delivery over passive targeting strategies. A second important parameter is nanoparticle size class, which determined both pace and amount of particle uptake where for large NPs saturation was reached quickly and for small NPs the uptake was the highest, but increased relatively slow during the observation time.

Considering difficulties during the washing procedure of the smallest NPs and the viscous plain chitosan coating solution, with substantial influence on NP size distributions as a consequence, together with the difficulties of dispersing the freeze-dried CHIT-coated NPs due to the remnants as seen on SEM pictures and the cytotoxicity caused by the combination of polymer H and plain chitosan; chitosan glutamate is suggested to be the better coating material for these Resomer® RG 503 H NPs. A drawback of Cglu-coated NPs are the lower zeta potential values, especially for Resomer® RG 503 NPs, which might indicate less stable colloidal properties and the lower pace in reaching maximum uptake values compared to plain chitosan. On the other hand, FITC degradation profiles of Cglu-coated NPs were very consistent in MFI reduction, independent of size and therefore, highly controllable. Moreover, for small polymer H Cglu-coated NPs cytotoxicity was negligible.

In conclusion, chitosan glutamate was shown to be a valuable alternative coating material for Resomer RG® 503 H PLGA nanoparticles compared to plain chitosan for the enhancement of nanoparticle-uptake in macrophages, the decrease in cytotoxicity and for establishing controlled release of its cargo inside the cell.

6. Acknowledgments

This research did not receive any specific grant from funding agencies in the public, commercial, or not-for-profit sectors.

- **Future Perspective:** (a speculative viewpoint on how the field will evolve in 5–10 years' time)

N/A

- **Executive Summary:** (bulleted summary points that illustrate the main conclusions made throughout the article. Less than 400 words).
  OR
  Summary Points (Research articles & Company profiles only): 8–10 bullet point sentences highlighting the key points of the article.

  - Nowadays, the need for particle-based drug delivery systems targeting macrophages is rising, as many infectious diseases and other physiological conditions are caused by the dysfunction of macrophages.
  - In this study, we assessed the influence of different formulation parameters e.g. incubation time, nanoparticle size class, polymer derivative, surface properties of PLGA nanoparticles on the uptake kinetics, degradation properties and cytotoxicity in macrophages.
  - Considering difficulties during the production of small chitosan-coated nanoparticles, with substantial influence on NP size distributions as a consequence, together with the difficulties of dispersing freeze-dried chitosan-coated nanoparticles, chitosan glutamate is suggested to be the better coating material.
  - A major enhancement in nanoparticle uptake resulted from altering the surface properties of PLGA nanoparticles by both chitosan coatings, especially when the core consisted of Resomer® RG 503 H. However, chitosan showed higher uptake rates compared to chitosan glutamate.
  - A second important parameter for cellular uptake is nanoparticle size class, where for large nanoparticles saturation of the cells was reached quickly, though for small NPs the uptake was the highest, but increased relatively slow during the observation time.
  - Chitosan coatings did not protect the PLGA core of the nanoparticles from degrading over time.
  - Fluorescein degradation profiles of chitosan glutamate-coated nanoparticles were consistent in mean fluorescence intensity reduction, independent of size and therefore, highly controllable.
  - The degradation of uncoated and plain chitosan-coated nanoparticles appeared to be size- and PLGA derivative-depended, where large particles and particles consisting of Resomer® RG 503 H

degraded more rapidly compared to small and medium sized nanoparticles or particles consisting of Resomer® RG 503.

- Cytotoxic properties of the nanoparticles were mainly caused by degradation products of large nanoparticles consisting of Resomer® RG 503 H, combined with plain chitosan.
- Toxicity was negligible for small sized nanoparticles, coated with chitosan glutamate as well as for nanoparticles consisting of Resomer® RG 503 and plain chitosan.

- **Figure/Table legends**

Figure 1: Scanning electron microscopy (SEM) images of different formulations of PLGA NPs. The scale bar indicating 2 µm is representative for all images, except for image C, where the scale bar represents 1 µm. Samples are coded by three formulation parameters: 1. The amount of stabiliser used, indicating size class (0.1 – 0.4 – 1) 2. The PLGA polymer used, indicating polymer H (Resomer® RG 503 H) or P (Resomer® RG 503) 3. The surface properties, indicating uncoated (NC), chitosan glutamate-coated (Cglu) or chitosan-coated (CHIT) NPs. Image (A) 0.1 H NC NPs (B) 0.1 H CHIT NPs (C) detail of 0.1 H CHIT showing possible chitosan remnants that cause aggregation of NPs, are indicated with an arrow. (D) 0.1 P NC NPs (E) 0.4 P Cglu NPs (F) 1 P CHIT NPs

Figure 2: Nanoparticle uptake profiles of all formulations. MFI is represented in function of the observation period of 24 hours, wherein distinction is based on surface properties: coating; the solid line represents NC NPs, the dotted line Cglu NPs and the dashed line CHIT NPs. (A) large NPs based on polymer P (B) middle-sized NPs based on polymer P (C) small NPs based on polymer P (D) large NPs based on polymer H (E) middle-sized NPs based on polymer H (F) small NPs based on polymer H. Average MFI was calculated over 7 repeats, error bars represent standard deviations.

Figure 3: Nanoparticle uptake profiles of all formulations. Number of fluorescent cells (%) is represented in function of the observation period of 24 hours, wherein distinction is based on surface properties: coating; the solid line represents NC NPs, the dotted line Cglu NPs and the dashed line CHIT NPs. (A) large NPs based on polymer P (B) middle-sized NPs based on polymer P (C) small NPs based on polymer P (D) large NPs based on polymer H (E) middle-sized NPs based on polymer H (F) small NPs based on polymer H. Average MFI was calculated over 7 repeats, error bars represent standard deviations.

Figure 4: Fluorescence microscopy images of nanoparticle uptake in macrophages. Colours indicate DAPI-stained blue cell nucleus, red phalloidin-stained actin filaments right beneath the cell membrane and green FITC-containing nanoparticles. Cells were incubated at 37°C or 4°C for 0 hours, 1 hour and 6 hours with different types of nanoparticles, represented in rows. The scale bar within the picture of the negative control indicates 10 µm.

Figure 5: MFI degradation profiles of the stability of the FITC signal inside macrophages over a 7 days observation period. A persistent signal is observed for all NP formulations in contrast to the FITC control. All formulations are represented in either (A) Uncoated NPs (B) Cglu coated NPs (C) CHIT coated NPs and controls; distinguished by polymer type (colour) and particle size class (line). Average MFI was calculated over 3 repeats, error bars represent standard deviations.

Figure 6: Representation of reduction in MFI (%). The difference in fluorescence between the maximum value and the end point, of all formulations. A trend, comparable to the multiple linear regression model, could be observed, where large NPs tend to give higher MFI reduction values compared to middle-sized and small-sized NPs. However, Cglu coated NPs had a relatively consistent MFI reduction, independently of size class. Average MFI reduction was calculated over 3 repeats, error bars represent standard deviations.

Figure 7: Representation of metabolising cells (%) after 24 hours incubation time with different formulations of PLGA NPs. A concentration of 2.7 mg/mL PLGA NPs was applied. The significant interaction effect between surface and polymer is clearly present as the viability of H CHIT NPs is lower compared to the other formulations. Another significant interaction was size class vs polymer, where 0.1 H NPs showed to be diminished compared to 1 H NPs. It has to be noted that for P NC NPs no decrease in cell viability was found, as oppositely for all Cglu NPs where cell viability was impaired. Stars represent significant differences (p-value < 0.05* or p-value <0.01**) according to unpaired two-tailed t-testing against the control group. Average of metabolising cells (%) was calculated over 3 repeats, error bars represent standard deviations.

Table 1: Overview of characteristics of all nanoparticle formulations. Results were calculated as the mean of all measurements of the three badges followed by the standard deviations. Samples are coded by three formulation parameters: 1. The amount of stabiliser used, indicating size class (0.1 – 0.4 – 1) 2. The PLGA

716 polymer used, indicating polymer H (Resomer® RG 503 H) or P (Resomer® RG 503) 3. The surface
717 properties, indicating uncoated (NC), chitosan glutamate-coated (Cglu) or chitosan-coated (CHIT) NPs.

718 • **References:** (visit our for authors page for formatting requirements and to download our citation style files)

719 1. Shapouri-Moghaddam A, Mohammadian S, Vazini H, *et al.* Macrophage plasticity, polarization,
720 and function in health and disease. *J. Cell. Physiol.* 233(9), 6425–6440 (2018).

721 2. Pei Y, Yeo Y. Drug delivery to macrophages: Challenges and opportunities. *J. Control. Release*.
722 240(May), 202–211 (2016).

723 3. Li Z, Xiong F, He J, Dai X, Wang G. Surface-functionalized, pH-responsive poly(lactic-co-glycolic
724 acid)-based microparticles for intranasal vaccine delivery: Effect of surface modification with chitosan
725 and mannan. *Eur. J. Pharm. Biopharm.* 109, 24–34 (2016).

726 4. Silva AL, Soema PC, Slütter B, Ossendorp F, Jiskoot W. PLGA particulate delivery systems for
727 subunit vaccines: Linking particle properties to immunogenicity. *Hum. Vaccines Immunother.* 12(4),
728 1056–1069 (2016).

729 5. Pei Y, Mohamed MF, Seleem MN, Yeo Y. Particle engineering for intracellular delivery of
730 vancomycin to methicillin-resistant Staphylococcus aureus (MRSA)-infected macrophages. *J. Control.*
731 *Release*. 267(July), 133–143 (2017).

732 6. Gong Y, Chowdhury P, Midde NM, Rahman MA, Yallapu MM, Kumar S. Novel elvitegravir
733 nanoformulation approach to suppress the viral load in HIV-infected macrophages. *Biochem. Biophys.*
734 *Reports*. 12(October), 214–219 (2017).

735 7. Jiang L, Greene MK, Insua JL, *et al.* Clearance of intracellular Klebsiella pneumoniae infection
736 using gentamicin-loaded nanoparticles. *J. Control. Release*. 279(January), 316–325 (2018).

737 8. Afzal I, Sarwar HS, Sohail MF, *et al.* Mannosylated thiolated paromomycin-loaded PLGA
738 nanoparticles for the oral therapy of visceral leishmaniasis. *Nanomedicine*. 14(4), 387–406 (2019).

739 9. Andreu V, Larrea A, Rodriguez-fernandez P, Alfaro S *et al*. Matryoshka-type gastro-resistant
740 microparticles for the oral treatment of Mycobacterium tuberculosis. *Nanomedicine*. 14(6), 707–726
741 (2019).

10. Anselmo AC, Mitragotri S. Cell-mediated delivery of nanoparticles: Taking advantage of circulatory cells to target nanoparticles. *J. Control. Release*. 190, 531–541 (2014).

11. Jain NK, Mishra V, Mehra NK. Targeted drug delivery to macrophages. *Expert Opin. Drug Deliv.* 10(3), 353–367 (2013).

12. Pang L, Zhu Y, Qin J, Zhao W, Wang J. Primary M1 macrophages as multifunctional carrier combined with plga nanoparticle delivering anticancer drug for efficient glioma therapy. *Drug Deliv.* 25(1), 1922–1931 (2018).

13. Yong S-B, Song Y, Kim HJ, Ain QU, Kim Y-H. Mononuclear phagocytes as a target, not a barrier, for drug delivery. *J. Control. Release*. 259, 53– 61 (2017).

14. Patel B, Gupta N, Ahsan F. Particle engineering to enhance or lessen particle uptake by alveolar macrophages and to influence the therapeutic outcome. *Eur. J. Pharm. Biopharm.* 89, 163–174 (2015).

15. Badkas A, Frank E, Zhou Z, *et al.* Modulation of in vitro phagocytic uptake and immunogenicity potential of modified Herceptin®-conjugated PLGA-PEG nanoparticles for drug delivery. *Colloids Surfaces B Biointerfaces*. 162, 271–278 (2018).

16. Qi F, Wu J, Li H, Ma G. Recent research and development of PLGA/PLA microspheres/nanoparticles: A review in scientific and industrial aspects. *Front. Chem. Sci. Eng.* 13(1), 14–27 (2019).

17. Xu Y, Kim CS, Saylor DM, Koo D. Polymer degradation and drug delivery in PLGA-based drug–polymer applications: A review of experiments and theories. *J. Biomed. Mater. Res. - Part B Appl. Biomater.* 105(6), 1692–1716 (2017).

18. Paul P, Sengupta S, Mukherjee B, Shaw TK, Gaonkar RH, Debnath MC. Chitosan-coated nanoparticles enhanced lung pharmacokinetic profile of voriconazole upon pulmonary delivery in mice. *Nanomedicine*. 13(5), 501–520 (2018).

19. Durán V, Yasar H, Becker J, *et al.* Preferential uptake of chitosan-coated PLGA nanoparticles by primary human antigen presenting cells. *Nanomedicine Nanotechnology, Biol. Med.* 21, 102073 (2019).

20. Gamucci O, Bertero A, Gagliardi M, Bardi G. Biomedical Nanoparticles: Overview of Their Surface Immune-Compatibility. *Coatings*. 4(1), 139–159 (2014).

21. Grabowski N, Hillaireau H, Vergnaud J, *et al.* Surface coating mediates the toxicity of polymeric nanoparticles towards human-like macrophages. *Int. J. Pharm.* 482(1–2), 75–83 (2015).

22. Hermans K, Van Den Plas D, Everaert A, Weyenberg W, Ludwig A. Full factorial design, physicochemical characterisation and biological assessment of cyclosporine A loaded cationic nanoparticles. *Eur. J. Pharm. Biopharm.* 82(1), 27–35 (2012).

23. Guo C, Gemeinhart RA. Understanding the adsorption mechanism of chitosan onto poly(lactide-co-glycolide) particles. *Eur. J. Pharm. Biopharm.* 70(2), 597–604 (2008).

24. Joseph E, Singhvi G. Multifunctional nanocrystals for cancer therapy: A potential nanocarrier. In: Nanomaterials for Drug Delivery and Therapy. Alexandru Mihai Grumezescu (Ed.), Elsevier Inc., Amsterdam, Netherlands, 91–116 (2019)

25. Toorisaka E, Watanabe K, Hirata M. Development of Fine Poly(D,L-Lactic-Co-Glycolic Acid) Particles for Hydrophilic Drug Using a Solid-in-Oil-in-Water Emulsion. *J. Encapsulation Adsorpt. Sci.* 08(02), 59–70 (2018).

26. Dyawanapelly S, Koli U, Dharamdasani V, Jain R, Dandekar P. Improved mucoadhesion and cell uptake of chitosan and chitosan oligosaccharide surface-modified polymer nanoparticles for mucosal delivery of proteins. *Drug Deliv. Transl. Res.* 6(4), 365–379 (2016).

27. Lutsiak MC, Robinson DR, Coester C, Kwon GS, Samuel J. Analysis of poly(D,L-lactic-co-glycolic acid) nanosphere uptake by human dendritic cells and macrophages in vitro. *Pharm. Res.* 19(10), 1480–7 (2002).

28. Xiong S, Zhao X, Heng BC, Ng KW, Loo JSC. Cellular uptake of Poly-(D,L-lactide-co-glycolide) (PLGA) nanoparticles synthesized through solvent emulsion evaporation and nanoprecipitation method. *Biotechnol. J.* 6(5), 501–508 (2011).

29. Yoo J-W, Chambers E, Mitragotri S. Factors that Control the Circulation Time of Nanoparticles in Blood: Challenges, Solutions and Future Prospects. *Curr. Pharm. Des.* 16(21), 2298–2307 (2010).

30. Acharya S, Sahoo SK. PLGA nanoparticles containing various anticancer agents and tumour delivery by EPR effect. *Adv. Drug Deliv. Rev.* 63(3), 170–183 (2011).

31. He C, Hu Y, Yin L, Tang C, Yin C. Effects of particle size and surface charge on cellular uptake and biodistribution of polymeric nanoparticles. *Biomaterials*. 31(13), 3657–3666 (2010).

32. Lanao RPF, Jonker AM, Wolke JGC, Jansen JA, Van Hest JCM, Leeuwenburgh SCG. Physicochemical properties and applications of poly(lactic-co-glycolic acid) for use in bone regeneration. *Tissue Eng. - Part B Rev.* 19(4), 380–390 (2013).

33. Kapoor DN, Bhatia A, Kaur R, Sharma R, Kaur G, Dhawan S. PLGA: A unique polymer for drug delivery. *Ther. Deliv.* 6(1), 41–58 (2015).

34. Van De Ven H, Vermeersch M, Matheeussen A, *et al.* PLGA nanoparticles loaded with the antileishmanial saponin β-aescin: Factor influence study and in vitro efficacy evaluation. *Int. J. Pharm.* 420(1), 122–132 (2011).

35. Bitencourt C da S, Silva LB da, Pereira PAT, Gelfuso GM, Faccioli LH. Microspheres prepared with different co-polymers of poly(lactic-glycolic acid) (PLGA) or with chitosan cause distinct effects on macrophages. *Colloids Surfaces B Biointerfaces*. 136, 678–686 (2015).

36. Qie Y, Yuan H, von Roemeling CA, *et al.* Surface modification of nanoparticles enables selective evasion of phagocytic clearance by distinct macrophage phenotypes. *Sci. Rep.* 6(1), 26269 (2016).

37. Barros D, Lima SAC, Cordeiro-Da-Silva A. Surface functionalization of polymeric nanospheres modulates macrophage activation: Relevance in Leishmaniasis therapy. *Nanomedicine*. 10(3), 387–403 (2015).

38. Hirota K, Terada H. Endocytosis of Particle Formulations by Macrophages and Its Application to Clinical Treatment. *Mol. Regul. Endocytosis*. , 413–428 (2012).

- **Reference annotations**: authors should highlight 6–8 references that are of particular significance to the subject under discussion as **"* of interest"** or **"** of considerable interest"**, and provide a brief (1–2 line) synopsis.

2. Pei Y, Yeo Y. Drug delivery to macrophages: Challenges and opportunities. *J. Control. Release*. 240(May), 202–211 (2016).

* This review summarises various approaches to address challenges in drug delivery to macrophages such as cellular uptake

14. Patel B, Gupta N, Ahsan F. Particle engineering to enhance or lessen particle uptake by alveolar macrophages and to influence the therapeutic outcome. *Eur. J. Pharm. Biopharm.* 89, 163–174 (2015).

* Review discussing important characteristics of particle-based drug delivery systems in macrophages

17. Xu Y, Kim CS, Saylor DM, Koo D. Polymer degradation and drug delivery in PLGA-based drug–polymer applications: A review of experiments and theories. *J. Biomed. Mater. Res. - Part B Appl. Biomater.* 105(6), 1692–1716 (2017).

* Complete review on PLGA degradation, considering a great number of influential parameters

19. Durán V, Yasar H, Becker J, *et al.* Preferential uptake of chitosan-coated PLGA nanoparticles by primary human antigen presenting cells. *Nanomedicine Nanotechnology, Biol. Med.* 21, 102073 (2019).

** Study investigating the reason for enhanced uptake of chitosan-coated PLGA nanoparticles in macrophages

21. Grabowski N, Hillaireau H, Vergnaud J, *et al.* Surface coating mediates the toxicity of polymeric nanoparticles towards human-like macrophages. *Int. J. Pharm.* 482(1–2), 75–83 (2015).

** Extensive research of cytotoxicity of chitosan-coated PLGA nanoparticles in macrophages

23. Guo C, Gemeinhart RA. Understanding the adsorption mechanism of chitosan onto poly(lactide-co-glycolide) particles. *Eur. J. Pharm. Biopharm.* 70(2), 597–604 (2008).

** Excellent paper on technical details of chitosan adsorption onto PLGA surface